Hindawi
Geofluids
Volume 2020, Article ID 6357683, 17 pages
https://doi.org/10.1155/2020/6357683

Research Article

Simulation Analysis of Influencing Factors of Subsidence Based on Mining under Huge Loose Strata: A Case Study of Heze Mining Area, China

Xianxiang Zhu,[1,2] Wenquan Zhang,[1,2] Zaiyong Wang,[1,2] Chenghao Wang,[3] Wei Li,[1,2] and Changhao Wang[4]

[1]*College of Mining and Safety Engineering, Shandong University of Science and Technology, Qingdao 266590, China*
[2]*State Key Laboratory of Mining Disaster Prevention and Control, Qingdao 266590, China*
[3]*China Railway Jinan Bureau Group Co., Ltd., Jinan 250001, China*
[4]*Zaozhuang Beihang Machine Tool Innovation Research Institute Co. Ltd., Zaozhuang 266590, China*

Correspondence should be addressed to Wenquan Zhang; wenquanzhang415@163.com

Received 31 January 2020; Revised 30 April 2020; Accepted 21 May 2020; Published 12 June 2020

Academic Editor: Constantinos Loupasakis

Copyright © 2020 Xianxiang Zhu et al. This is an open access article distributed under the Creative Commons Attribution License, which permits unrestricted use, distribution, and reproduction in any medium, provided the original work is properly cited.

Based on the coal seam mining under the condition of thick soil layer, the mechanical mining subsidence process under the condition of thick soil layer was analyzed. Combined with the results of core drilling and laboratory test in the mining area, the mechanical analysis of the special transition strata of "hard soil-soft rock" at the bottom of the soil layer was carried out. Additionally, the characteristics of the shallow buried soil layer were compared and analyzed. Furthermore, the significance of this transitional font to the surface subsidence law was proposed. By using the numerical simulation software of FLAC^{3D} and choosing the thickness of "hard soil-soft rock" transitional font as the influencing factor, a model was established and the surface subsidence characteristics of different stratum combinations were numerically simulated. The research results show that the transitional font is the special strata indicating that the hard soil is transiting to the soft rock, having a significant effect on the ground movement and deformation induced by coal mining. It cannot be designated into the loose strata. Also, it cannot be regarded as the bed rock to study the influence of it on the surface subsidence. The "hard soil-soft rock" transitional font has the support effect on the overlying strata during coal seam mining, which can restrict the surface subsidence. Furthermore, the larger the thickness of the transitional font is, the more obvious the restricting effect of it on the surface subsidence is. Meantime, this restricting effect will not be changed with the variation of the proportion between the loss bed and the bed rock thickness. Only the restricting extent is a little different.

1. Introduction

In East China, Central China, and North China, the overburden bedrock above coal seams in mining areas is usually thin, whereas the unconsolidated layers are thick [1]. In the mining area of Heze in Shandong Province, China, the ultrathick unconsolidated layer has a thickness in the range 400 to 900 m, making the mining subsidence particularly different from that in other areas. The law of surface movement in the ultrathick unconsolidated layer under different mining and geological conditions has been studied by researchers both in China and abroad. Yang and Xia [2] used on-site measurement and artificial neural network prediction methods to study the deformation characteristics of settlement and motion caused by mining under thin bedrock and huge thick loose layer. The artificial neural network was used to study the mining subsidence under thin bedrock and huge thick loose layer. Quantitative predictions and improved artificial neural network output can reflect changes in ground motion and deformation. Wang et al. [3] analyzed the stability of bearing structures (arch structures in loose layers and key layers in rock formations), based on their effects on formation movement, revealing the formation mechanism of surface collapse and the role of two key

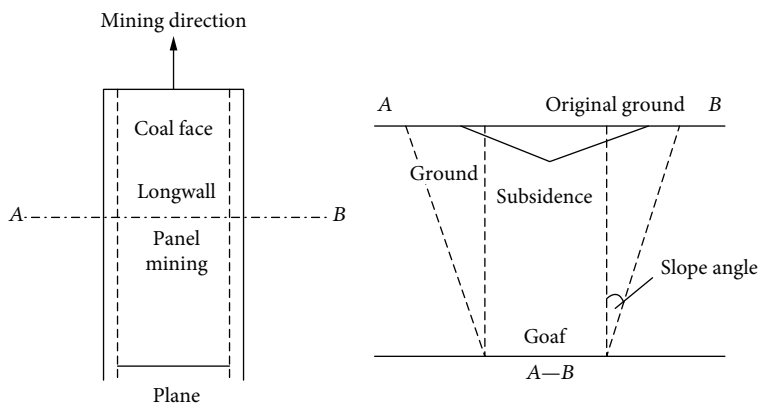

Figure 1: Mining mobile basin.

parameters: mining length and mining height, and a backfilling mining method is proposed to prevent the failure of the load-bearing structure by determining the appropriate length of the longwall face and the mining height to avoid surface collapse; Chai et al. [4] use a fiber optic sensing monitoring network to monitor surface movement and deformation and provide a new idea for preventing surface subsidence; Sun et al. [5] proposed a simulated hyperbolic subsidence method based on key layer theory and overburden mechanics analysis. The discrete element method (UDEC) was used to verify the movement of the rock caused by mining, and the performance of the theoretical model was evaluated. Based on the theory of rock rheology and probability integral method, Hou et al. [6] established a superposition model for predicting the dynamic settlement of the ground in the thick pine layer. Based on the comparison between the Huayi Zhaoyi Mine and the Zhaoer Mine, the surface of the thick loose layer mining control is controlled. Settling provides a reference. Li et al. [7] studied the influence of coal type on overburden and surface movement characteristics of combustion space, proposed the wellbore free UCG surface subsidence prediction method, and applied this method to the UCG industrial test site in Ulanqab. Xu et al. [8, 9] deduced the load transfer coefficient in composite hard rock and overburden rock from the stress-strain relationship in the thick unconsolidated layer; a geological mechanical model based on the specific geological conditions was introduced first, and then, numerical analyses of the load transfer mechanism of mining the overlaying rock in the working face of the thin bedrock and the deformation characteristic of the overlaying rock were carried out. The law of surface subsidence caused by mining under the thick unconsolidated layer, associated with a larger ground subsidence coefficient, and an extended subsidence trough, was quite different from that under other geological conditions. Also, due to the widely influenced area caused by mining under the thick unconsolidated layer and the sensitivity of ground deformation to the bedrock movement, the subsidence speed was faster and the active period of surface movement was longer, causing more serious damage to the above ground structures [10]. The influence of rock characteristics on surface subsidence and the corresponding prediction methods were also studied by other researchers [11–13]. However, few studies focused on the prediction of the surface subsidence caused by mining under the ultrathick unconsolidated layer, nor the effects of different soil conditions in the unconsolidated layer on the surface subsidence [14]. For the study of geological fluids, the study of mechanical properties is obtained through numerical simulation calculations [15, 16]. The law of surface subsidence caused by mining under the ultrathick unconsolidated layer was studied in this paper, which was based on the analyses of field data from the 1304N working face of a coal mine in Shandong Province, China. The results are of great significance to the study of effective control of surface subsidence caused by mining under the ultrathick unconsolidated layer and protection of above-ground structures.

2. Mechanism of Mining Subsidence in the Unconsolidated Layer

Mining subsidence is a mechanical phenomenon in overburden soil media in coal seams. In soil mechanics, underground goafs (i.e., mined-out areas) form under the soil layer when a coal seam is mined, and the overburden roof stratum moves due to the loss of support from this coal seam. The roof will fracture or fall if the additional stress caused by coal mining exceeds its strength limit, often causing a ground subsidence trough [17, 18], as shown in Figure 1.

With the loss of support from the lower coal seam, part of the weight will influence undisturbed soil when the rock layer moves and deforms, causing the stress of rock near goafs to change and redistribute, creating an elevated stress zone and a reduced stress zone, as shown in Figure 2.

During excavation in the working face, the boundary coal pillars and the upper strata, which are in the abutment pressure zone, along with the additional stress, will gradually influence the ground. As the mining depth increases, the influence caused by mining on the ground will become reduced [19].

Surface subsidence curve analysis shows that the subsidence results from the collapse of overburden soil and the displacement caused by compaction and consolidation deformation (Figure 3). In the coal seam with an overburden unconsolidated layer, compaction and consolidation

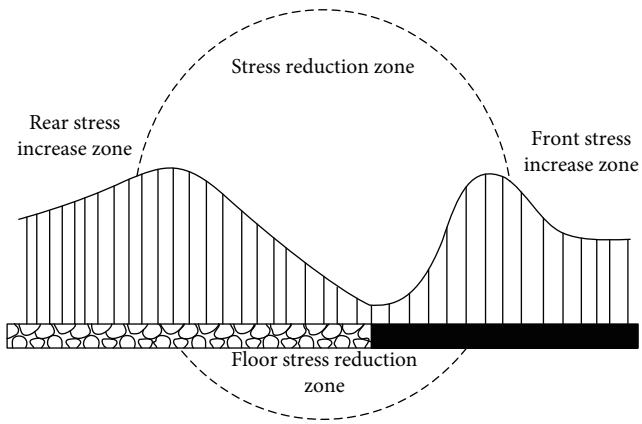

Figure 2: Mining stress distribution.

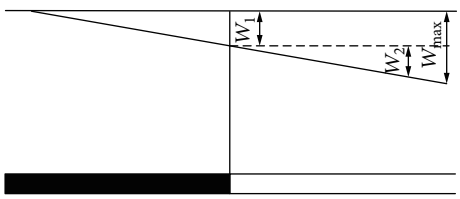

Figure 3: Surface sinking curve.

deformation of the layer should be considered in the study of the surface subsidence caused by mining. The mining-caused surface subsidence includes two parts.

$$W_{max} = W_1 + W_2, \tag{1}$$

where W_1 is the general bottom subsidence. When the coal mining is completed, overburden soil will collapse under its self-weight and the subsidence will gradually transfer to ground to some extent, which is W_1.

According to mining subsidence theory, W_1 is calculated by

$$W_1 = Mq, \tag{2}$$

where q is the subsidence factor (less than the thickness of coal mining, i.e., $q < 1$), M is the thickness of mining, and W_1 is the subsidence.

The compression of the overburden soil layer and the coal seam caused by mining is usually negligible. W_2 is the subsidence caused by consolidation, which is mainly due to water loss and soil compaction in the unconsolidated layer.

The common equations for maximum subsidence are as follows:

(1) When the coal seam is horizontal,

$$W_{max} = Mq \tag{3}$$

(2) When the coal seam is inclined,

$$W_{max} = Mq \cos \alpha, \tag{4}$$

where q is the subsidence factor (less than the thickness of coal mining, i.e., $q < 1$), M is the thickness of mining, α is the angle of incline (°), and W_{max} is the maximum subsidence of full mining [20] (m)

For nonfull mining, the calculation of maximum subsidence should take into account not only the coal thickness, the subsidence factor, and the angle of incline but also the mining area, which has a big influence on the subsidence. Two empirical equations are usually used to calculate the maximum subsidence for nonfulling mining.

(1) The first empirical equation is

$$W_{fm} = Mq \cos \alpha \sqrt{n_1 \cdot n_3}, \quad n_1 = K_1 \frac{D_1}{H_1}, n_3 = \frac{D_3}{H_0}, \tag{5}$$

where n_1 and n_3 are the mining factors, K_1 and K_3 are factors less than 1, D_1 and D_3 are the dip length and strike length of the working face (m), H_0 is the average mining depth (m), and W_{fm} is the maximum subsidence for nonfull mining (m)

(2) The second empirical equation is

$$W_{fm} = M\left[1 - e^{-\rho(D_1/H_0)^2}\right], \tag{6}$$

where ρ is the factor related to overburden rock type.

$\rho = 1$ when the overburden stratum is hard rock; $\rho = 2$ when the overburden stratum is medium hard; and $\rho = 3$ when the overburden stratum is subjected to repeated mining

3. Analysis of Mechanical Properties of the Ultrathick Unconsolidated Layer

Mining in the ultrathick unconsolidated layer is categorized as mining under special geological conditions. Unconsolidated layers are usually quaternary and tertiary nondiagenetic sedimentary rock and have a large impact on the ground movement and its characteristics.

According to the general deposition pattern, the thickness of the unconsolidated layer increases over the deposition time, as well as the complexity of its structure. The properties and structure characteristics will also change over time [21, 22]. Zhang [23] studied the hard soil/soft rock (a new type of soil) and found a well-developed zone at the bottom of the unconsolidated layer. This is a gradually changing and indistinct zone, which is termed the hard soil/soft rock special transition zone. The special transition zone in the unconsolidated layer should be differentiated; otherwise, error will be induced by classifying it as an unconsolidated layer or bedrock.

3.1. Relationship between the Coefficient of Compression and the Depth. The coefficient of compression [24] is an index that describes the compressibility of soil. Several clay core samples, which were from unconsolidated layers of PS1 in Pengzhuang Coal Mine and SX1 and SX2 in Guotun Coal Mine, were tested in laboratory tests. As shown in Figure 4,

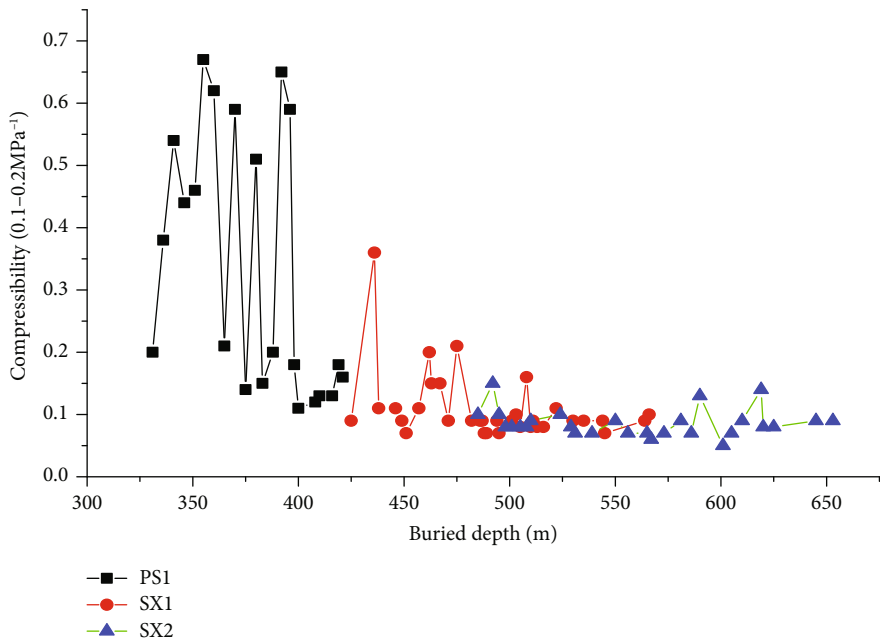

Figure 4: Clay compression coefficient and burial depth curve.

when the depth is less than 450 m, the coefficients of compression are scattered and large with the highest value of 0.67; when the depth is more than 450 m, the coefficients of compression show a clear decrease and are close to 0.09 as the depth increases.

The deeper the clay layer is, the longer deposition history it has and the better it is developed, and the resistance to deformation becomes considerably large. The clay is regarded as having the strength of soft rock. Therefore, the clay layer at a larger depth is developing toward soft rock, forming a transition phase. Due to its large strength and the support it provides for the overburden soil layer, the clay layer has a big impact on the surface subsidence.

3.2. Analysis of the Compression Strength of Soil in the Unconsolidated Layer. The unconfined compression strength of silty clay at shallow depth is in the range 40 to 140 kPa, whereas the unconfined shear strength of clay is in the range 60 to 180 kPas shown in Figure 6, a. In ultrathick unconsolidated layers, the shear strength of clay is much larger than 180 kPa with the largest value of 1529 kPa. This means the degree of consolidation of clay becomes larger as the depth increases, its compression strength is way larger than that of normal clay, and its bearing capacity becomes remarkably larger. According to Zhang et al. [25], hard soil/soft rock has an axial compression strength in the range 0.3 to 1.5 MPa. Thus, the layer in this study is a typical special transition zone in hard soil/soft rock, which supports the overburden strata and eliminates part of the additional stress caused by mining, and finally restrains the surface subsidence [26].

3.3. Analysis of the Shear Strength of the Unconsolidated Layer. The shear strength [27–29], which is reflected by the angle of friction and the cohesion of soil and rock, is a very important property in rock mechanics. The laboratory tests

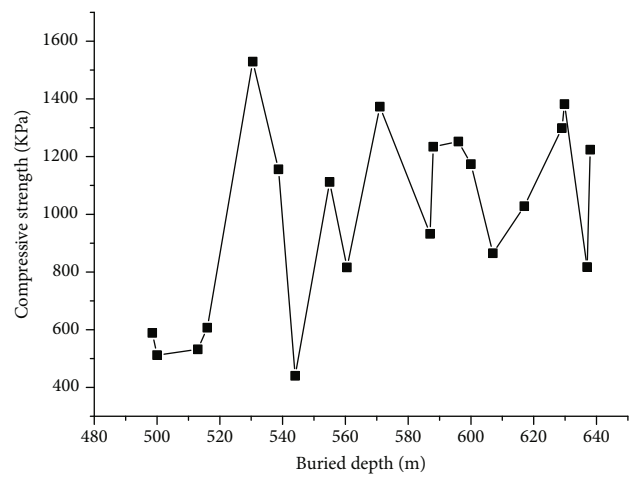

Figure 5: Curve of compressive strength and depth of deep clay in Neogene.

are usually conducted to indirectly predict the shear strength through finding the angle of friction and the cohesion. It is thus of great importance to study the angle of friction and the cohesion of the unconsolidated layer.

The cohesion of clay in Figure 6 is relatively low at a shallow depth, with an average of 40 kPa; it increases with the depth and stays stable at around 140 kPa when depth is more than 450 m.

The angle of friction in Figure 7 increases and stays stable at around 20° at the depth of 450 m.

The distinct change in clay parameters at the depth of 450–475 m means the properties of clay are different from those at a shallow depth. This depth is the critical depth at which clay consolidates into rock and behaves as rock. Such clay can be regarded as typical hard soil/soft rock.

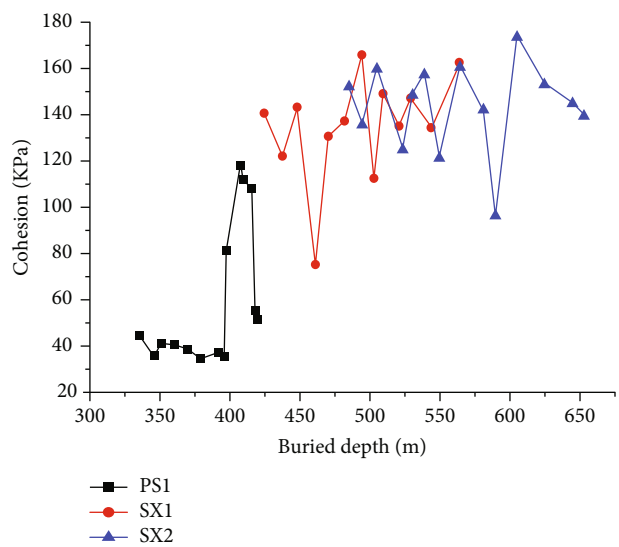

Figure 6: Curve of cohesion and depth of deep clay in Neogene.

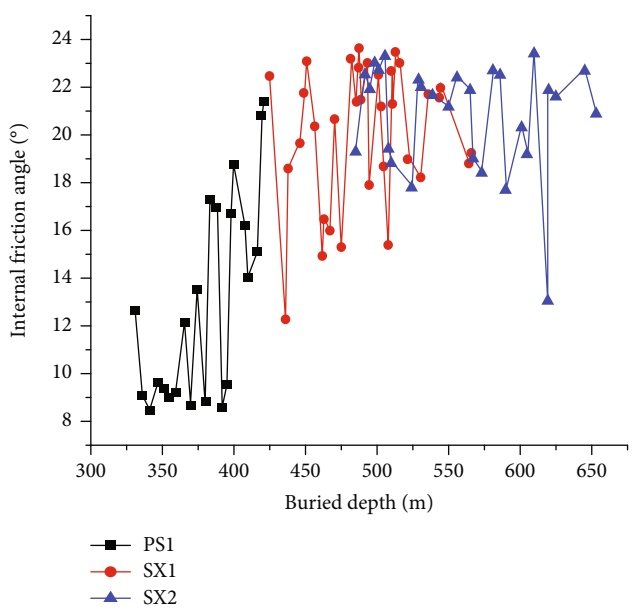

Figure 7: Curve of internal friction angle and depth of deep clay in Neogene.

4. Simulation and Analysis of Mining Subsidence Laws of Mining in the Thick Unconsolidated Layer

4.1. Model Building and Mechanical Parameters. Geological conditions and stratum conditions were modeled in FLAC 3D, with meshes at every 5 m in the X and Y coordinates. The model is shown in Figure 8.

In view of this numerical simulation study, in order to reveal the research on the ground subsidence law of mining under huge thick loose layers, combined with the foregoing, it is determined that the thickness of the "hard soil-soft rock" transition body, the thickness of the loose layer, and the thickness of the bedrock are simulated variables. Control a single variable, analyze the three factors one by one, and study the effect of different thickness on the surface subsidence law. The thickness of the "hard soil-soft rock" transition body is divided into six grades of 70 m, 90 m, 110 m, 130 m, 150 m, and 170 m, respectively. The thickness of the loose layer is divided into six grades of 350 m, 400 m, 450 m, 500 m, 550 m, and 600 m. The rock thickness is divided into six grades: 50 m, 60 m, 70 m, 80 m, 90 m, and 100 m; in addition, a total of 27 models are designed when the burial depth is controlled to be at a certain amount; a total of 27 models are established in the model.

The boundary conditions are shown in Figure 9: a strike length of 600 m in the working face, a working face length of 150 m, and a thickness of 10 m in coal mining, with an excavation step of 40 m. The subject sections are the centers of subsidence trough and vertical trough, with the same strike as the mining direction. The observation points were selected at the top of the main section, with an interval of 40 m and 50 in total. At the same location of the bedrock in the model, the displacement observation points were selected with an interval of 40 m and 50 in total too. The difference of the subsidence of ground and the bedrock was compared, the movement of the unconsolidated layer as the soil conditions change as well as the changing trend of compression was studied, and then, the subsidence laws caused by the unconsolidated layer were analyzed. The physical and mechanical properties are shown in Table 1, and simulation programs are in Table 2.

4.2. Analysis of Effects of the Hard Soil/Soft Rock Thickness on the Surface Subsidence. Results of the subsidence curves of every condition from the 50 observation points in programs 1 and 2 (Table 2) are shown in Figure 10.

The subsidence factors under different conditions were calculated using the empirical equations, which are shown in Figure 11.

The subsidence factors and vertical subsidence, as shown in Figures 10–12, gradually reduce as the transition areas increase. This phenomenon is related to the properties of the transition zone [30]. The transition zone differs from the unconsolidated layer and the bedrock: it is a transition zone between soil and rock, and it has the characteristics of both soil and rock in terms of composition, structure, and formation.

When it is mined, the transition zone has more resistance to disturbance than the overburden unconsolidated layer and provides support and buffering when the unconsolidated layer deforms, resulting in a remarkable decrease in the surface subsidence.

4.3. Analysis of the Unconsolidated Layer Thickness. The surface subsidence of the unconsolidated layer was simulated in program III, which is shown in Figure 13.

The mining depth increases with an increasing thickness of the unconsolidated layer, and the surface subsidence trough will also extend. A trend of increasing before decreasing of the maximum subsidence and the subsidence factors is mainly due to the unconsolidated layer itself.

During mining in the ultrathick unconsolidated layer, the coal seam is unable to provide enough support for the

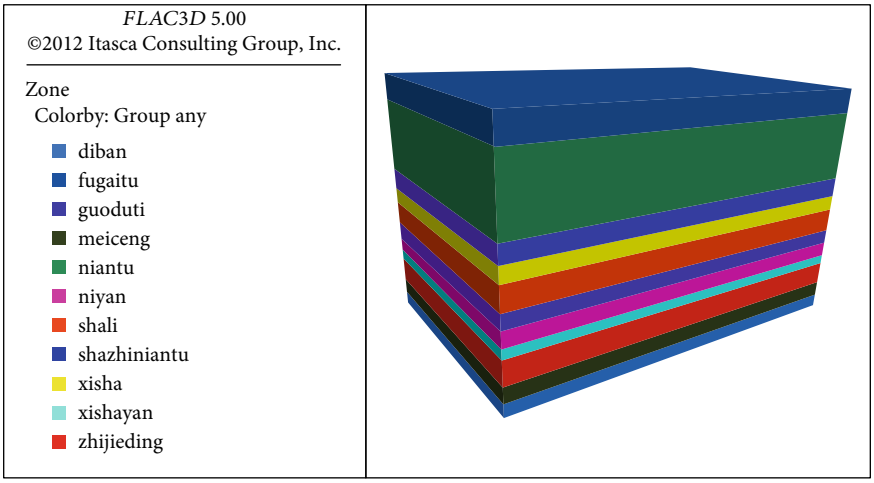

Figure 8: Schematic diagram of FLAC model.

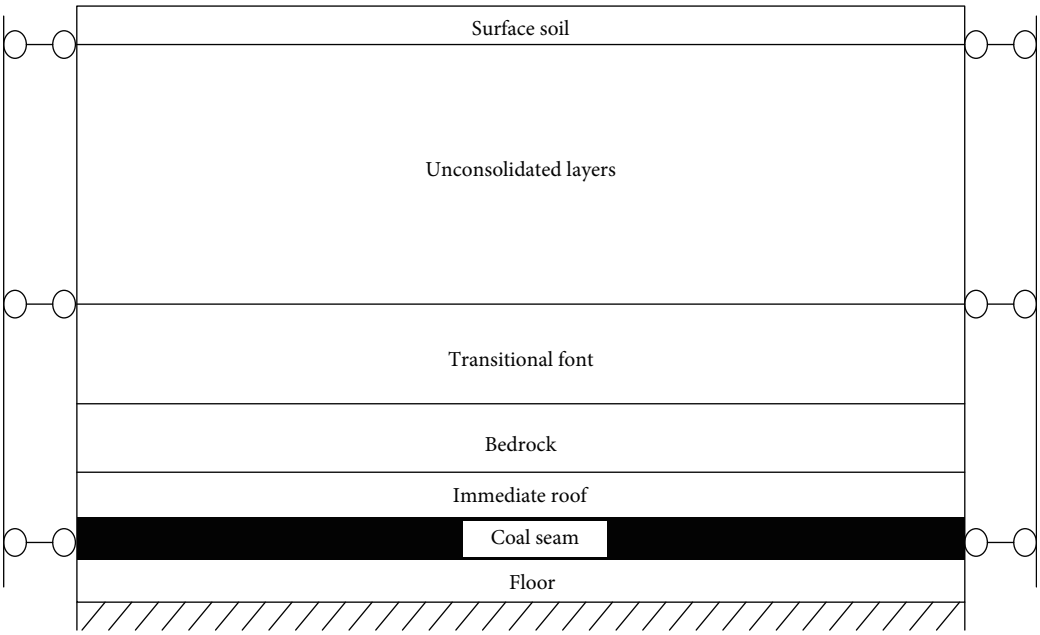

Figure 9: Schematic diagram of working face geological model.

Table 1: Numerical simulation of material mechanics parameters.

Serial number	Stratum	Bulk modulus (MPa)	Shear modulus (MPa)	Cohesion (MPa)	Internal friction angle (°)	Tensile strength (MPa)	Density (kg·m^{-3})
1	Covered soil	16.7	5.4	0.12	17	0	1875
2	Clay	22	16.5	0.15	18	0	1960
3	Sandy clay	26.5	17	0.16	18	0	1975
4	Fine sand	33.5	17.5	0.14	18	0	1985
5	Gravel	35	19	0.14	19	0	1945
6	Transitional font	27.5	165	0.17	22	0.86	2150
7	Mudstone	33	1350	2.30	34	1.63	2600
8	Fine sandstone	3750	1350	6.50	39	2.45	2300
9	Immediate roof	2850	1450	2.85	31	2.40	2550
10	Coal seam	1900	1200	2.15	32	2.25	1450
11	Floor	4250	2600	3.30	37	3.55	2600

Table 2: Simulation scheme.

Program	Model number	Thickness of loss bed (m)	Bedrock thickness (m)	Transitional font thickness (m)
I	1	400	60	70
	2	400	60	90
	3	400	60	110
	4	400	60	130
	5	400	60	150
	6	400	60	170
II	7	350	70	70
	8	350	70	90
	9	350	70	110
	10	350	70	130
	11	350	70	150
	12	350	70	170
III	13	350	50	70
	14	400	50	70
	15	450	50	70
	16	500	50	70
	17	550	50	70
	18	600	50	70
IV	19	450	50	110
	20	450	60	110
	21	450	70	110
	22	450	80	110
	23	450	90	110
	24	450	100	110
V	25	400	160	0
	26	400	50	110
	27	510	50	0

overburden soil because the bedrock and the transition zone are relatively thin. Thus, the additional stress will induce the compression of soil, and the pore volume will decrease due to water being squeezed out of the unconsolidated layer, causing the consolidation deformation and then surface subsidence to develop.

When the thickness of the unconsolidated layer is as large as a certain value, the soil will have enough resistance to the impact of additional stress and thus decrease the surface subsidence.

4.4. Analysis of the Bedrock Thickness. Based on the field data from several coal mining areas, the surface subsidence of bedrock of different thickness was simulated. The maximum subsidence in six cases is shown in Figure 14.

The maximum surface subsidence and the subsidence factors will decrease as the thickness of the bedrock increases. This is caused by the insufficient support from the thin bedrock to the overburden strata, and large surface subsidence takes place. However, an effective stress that supports strata (key strata) will occur as the thickness of the bedrock increases. It provides an effective constraint on the deformation of the overburden strata, and the surface subsidence will be gradually reduced as the thickness of the bedrock increases.

4.5. Compression Analysis of the Unconsolidated Layer. A numerical model was used to study the impacts of the hard soil/soft rock transition zone, the unconsolidated layer, and the bedrock on compression. Subsidence curves of the bedrock roof are shown in Figure 15, which consist of the data obtained from the 50 observation points.

The subsidence curve of bedrock roof is similar to the surface subsidence in Figure 15, with the maximum subsidence occurring above the central point of the mining area, from which the curve shows a symmetric distribution.

The maximum compression of the unconsolidated layer can be expressed as the difference of the maximum surface subsidence and the maximum bedrock subsidence. The compression was calculated and is shown in Figures 16.

As shown in Figure 16, the bedrock effectively constrains the subsidence of overburden strata and the constraint effect intensifies as the thickness of the bedrock increases, reducing the additional stress in the unconsolidated layer and thus resulting in less compression.

In the first program, the transition zones increase at intervals of 50 m. The maximum and minimum decreases in compression between two adjacent models are 0.41 and 0.18 m, with an average value of 0.31 m. In the second program, the transition zones also increase at intervals of 50 m. The maximum and minimum decreases in compression between two adjacent models are 0.32 and 0.18 m, with an average value of 0.27 m. In the fourth program, the transition zones increase at intervals of 10 m. The maximum and minimum decreases in compression between two adjacent models are 0.67 and 0.27 m, with an average value of 0.44 m.

The impact of the transition zone on the compression of the unconsolidated layer is less than that of the bedrock in terms of the decrease in compression, which shows that the hard soil/soft rock transition zone is the special strata between soil and rock.

The fitting equation describing the compression is also shown in Figure 17. Analyses of these four simulations show that the hard soil/soft rock transition zone constrains the compression of the unconsolidated layer.

4.6. Boundary Angle. The boundary angle is the angle formed when a line formed by points (which have a subsidence of 10 mm in the subsidence trough) intersects the horizontal line on the coal pillar. This is the general definition of boundary angle when full mining or near full mining are involved. The determination of the boundary angle will change when the unconsolidated layer exists. To determine the boundary angle, a line should be drawn from the boundary points in the trough as the unconsolidated layer displacement angle line, which intersects the layer between the bedrock and the unconsolidated layer. Then another line is formed by connecting this intersection with the mining boundary, and the boundary angle is formed when this line intersects the horizontal line in the coal pillar.

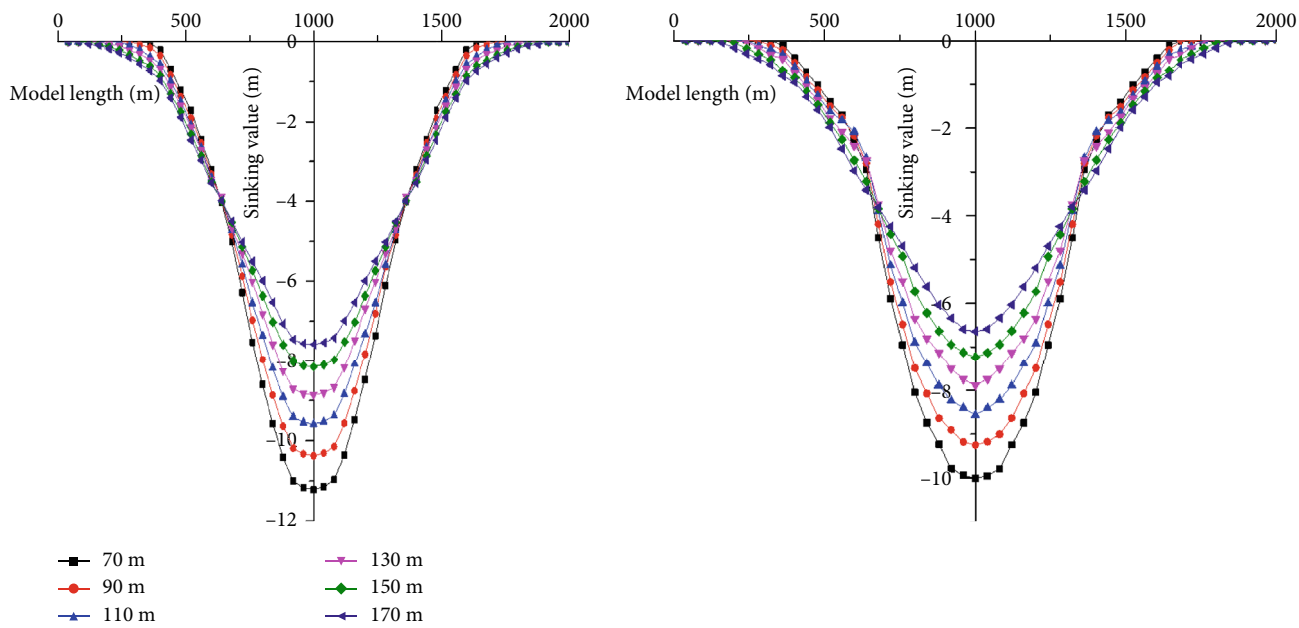

Figure 10: Surface sinking curve with different transitional font thickness.

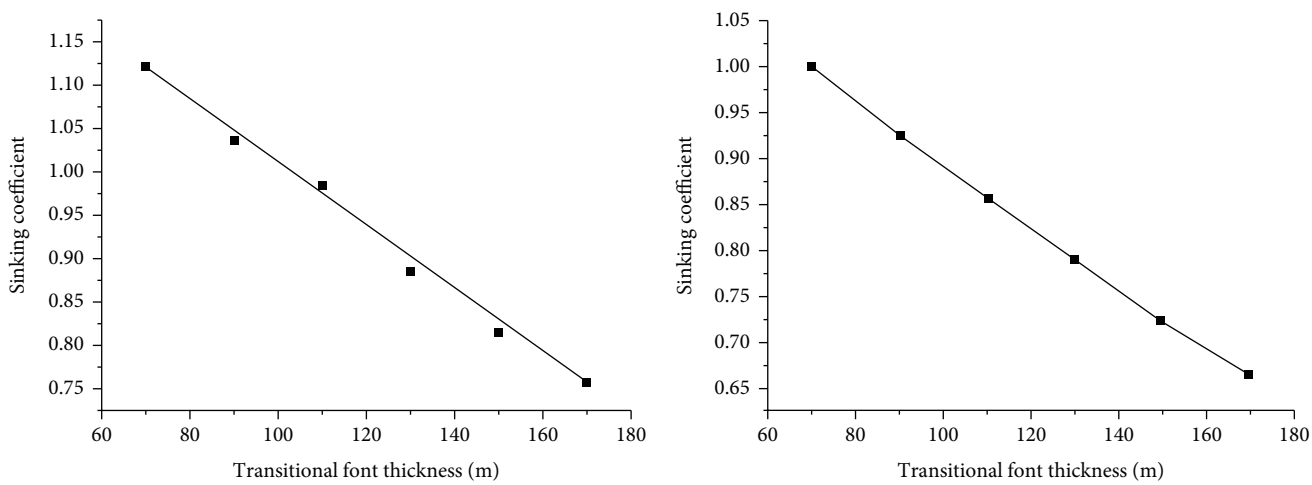

Figure 11: Variation of sinking coefficient of different transitional font thickness.

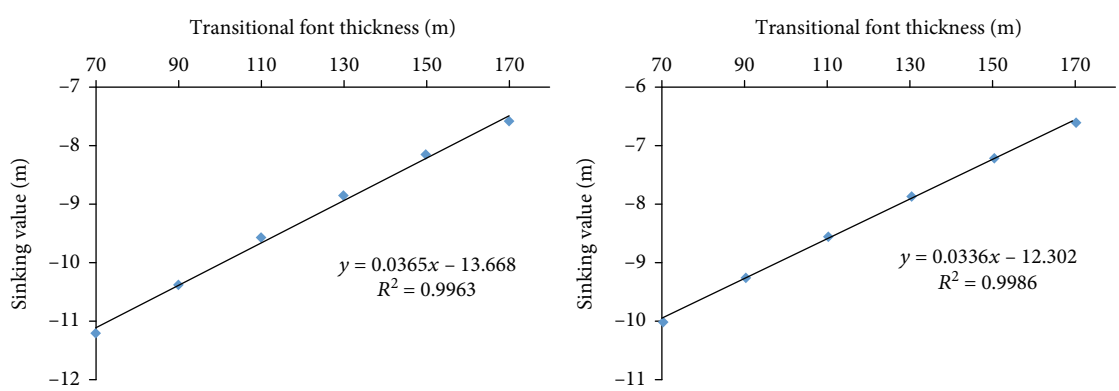

Figure 12: Fitting value and transition body thickness fitting equation curve.

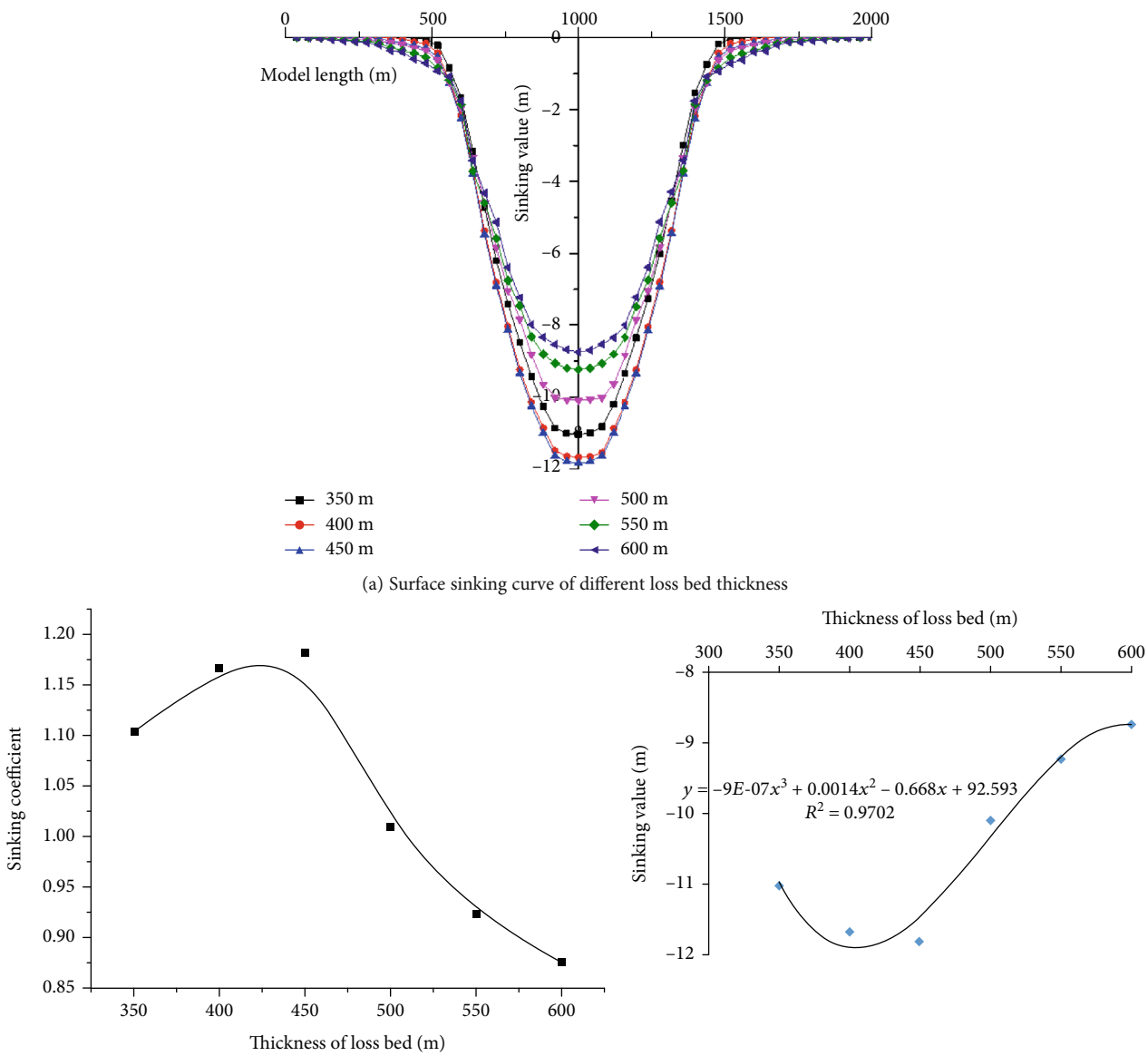

(a) Surface sinking curve of different loss bed thickness

(b) Variation of sinking coefficient of different loss bed thickness

(c) Sink value and loss bed thickness correlation curve

Figure 13: Different loss bed thickness affects sinking.

The boundary angles are usually different in various soil conditions. Deng et al. [31] studied the influences of the hard soil/soft rock transition zone, the unconsolidated layer, and the bedrock on the boundary angle separately. When there is a hard soil/soft rock transition zone in the strata, the boundary angles of the unconsolidated layer, the hard soil/soft rock transition zone, and the bedrock should be calculated separately.

The boundary angles of the unconsolidated layer, the hard soil/soft rock transition zone, and the bedrock are assumed to be $\varphi 0$, $\theta 0$, and $\delta 0$ (Figure 18). The property of transition zone can be shown through the differences of boundary angles in the unconsolidated layer, hard soil/soft rock transition zone, and the bedrock, and the properties can be studied quantitatively.

The depth of the coal in this study was chosen to be 560 m, the boundary angles of hard soil/soft rock transition zone were calculated based on the subsidence isochron of 10 mm in five simulation programs.

In the result of program V, the points with a final subsidence of 10 mm were selected and indicated in Table 3.

$$\begin{aligned} \frac{400}{\tan\varphi_0} + \frac{160}{\tan\delta_0} &= 700 - 177.4 = 522.6\,\text{m}, \\ \frac{400}{\tan\varphi_0} + \frac{110}{\tan\theta_0} + \frac{50}{\tan\delta_0} &= 700 - 151.9 = 548.1\,\text{m}, \\ \frac{510}{\tan\varphi_0} + \frac{50}{\tan\delta_0} &= 700 - 118.1 = 581.9\,\text{m}. \end{aligned} \tag{7}$$

Solving this equation, $\varphi 0 = 42.6^\circ$, $\theta 0 = 52.1^\circ$, and $\delta 0 = 61.3^\circ$.

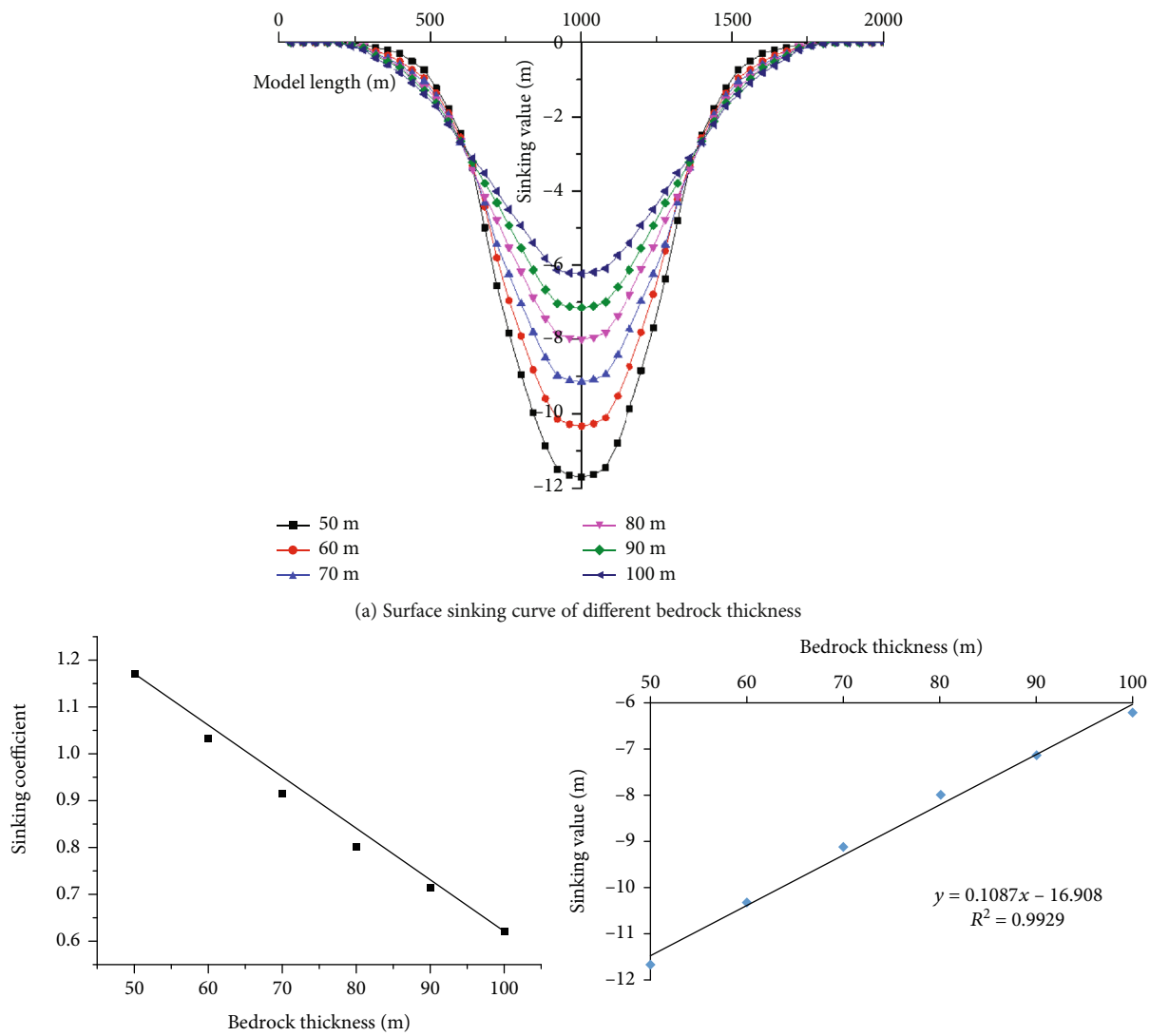

(a) Surface sinking curve of different bedrock thickness

(b) Variation of sinking coefficient of different bedrock thickness

(c) Subsidence value and bedrock thickness correlation curve

Figure 14: Different bedrock thickness affects sinking.

The boundary angles of the unconsolidated layer, the hard soil/soft rock transition zone, and the bedrock are 42.6°, 52.1°, and 61.3°.

Different strata have different boundary angles, and the boundary angle is proportional to the strength of the strata.

The boundary angle of the transition zone, which is 52.1°and in the range 42.6° (in the unconsolidated layer) to 61.3° (in the bedrock), indicates the strength of the transition zone is between the unconsolidated layer and the bedrock and confirms the transition from hard soil to soft rock and its influence on the surface subsidence.

5. Sensitivity Analysis Based on the Fuzzy Neural Network

5.1. Setup of the Mathematical Model. The neural network model built on the neural network toolbox of the MATLAB platform includes three input layer units, which represent the three main control factors that affect the maximum surface subsidence value studied in the previous article; one output layer, which indicates the maximum surface subsidence implicit. The number of neurons in the layer is determined to be 7; the momentum and adaptive gradient decreasing training function traingdx are selected; the step size is 0.2; the momentum factor is 0.9; the initial network weight is set to a fixed value; the learning rate is 0.05; the expected error is 0.001. The maximum training period is 100,000. The mechanism function selects logsig-purelin. The performance function selects the weighting function mesereg.

The relationship between the neurons of the neural network can be obtained by running the established neural network learning algorithm. To get the actual connection between the input factors and the output factors, that is, the weight of the influence of the input factors on the output factors, the weights are processed. To this end, the following indicators are introduced to describe the relationship between input factors and output factors [32–34].

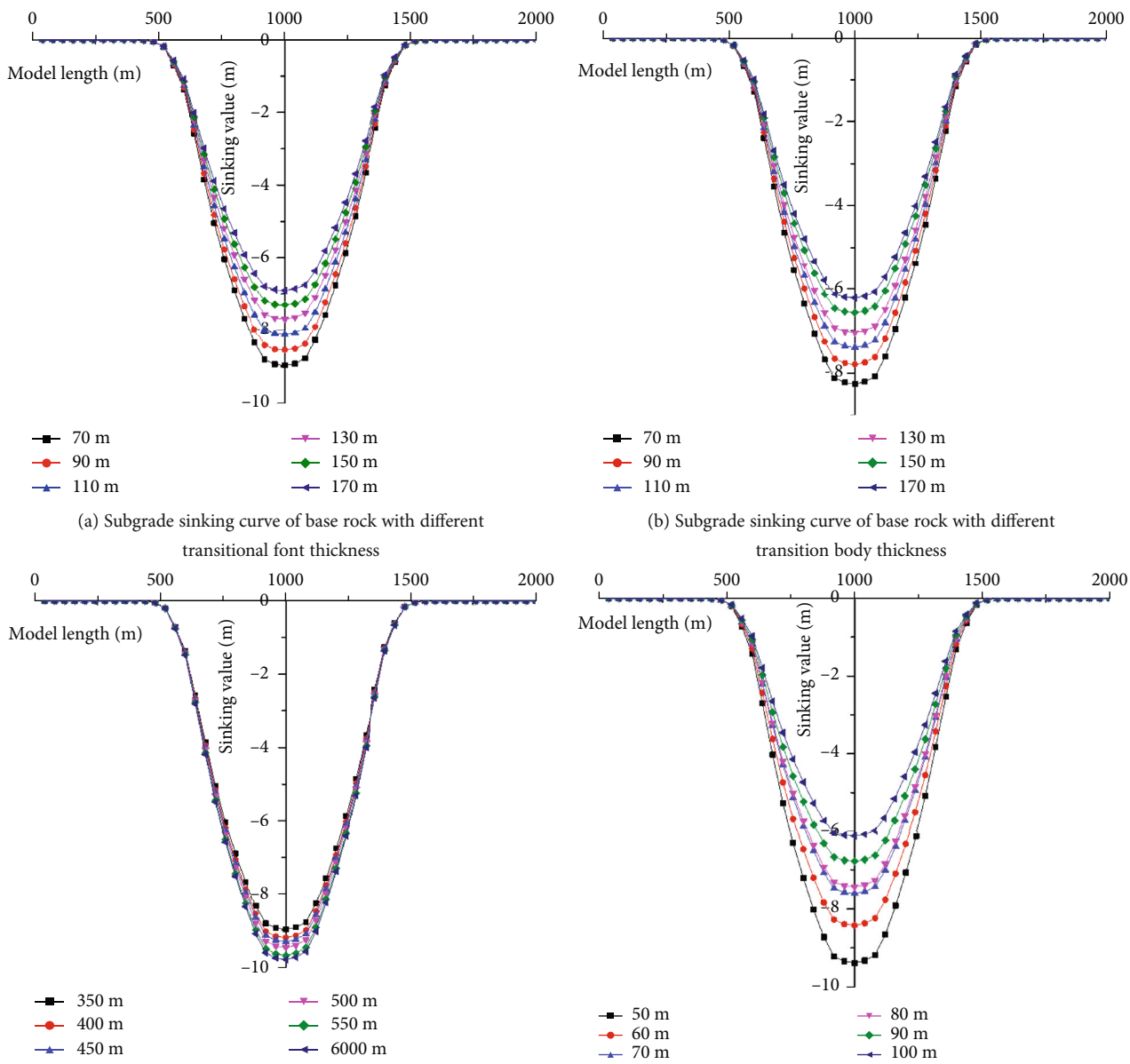

(a) Subgrade sinking curve of base rock with different transitional font thickness

(b) Subgrade sinking curve of base rock with different transition body thickness

(c) Submarine sinking curve of different loss bed thickness bedrock

(d) Subgrade sinking curve of base rock with different bedrock thickness

Figure 15: Subgrade sinking curve of bedrock with different stratum thickness.

(1) Correlation significance coefficient:

$$r_{ij} = \sum_{k=1}^{P} W_{ki} \frac{1 - e^{-X}}{1 + e^{-X}}, \quad X = \omega_{jk}. \tag{8}$$

(2) Correlation index:

$$R_{ij} = \left| \frac{1 - e^{-y}}{1 + e^{-y}} \right|, \quad y = r_{ij}. \tag{9}$$

(3) Absolute influence factor

$$S_{ij} = \frac{\mathrm{R}_{ij}}{\sum_{i=1}^{m} R_{ij}}. \tag{10}$$

where i is the input unit of the neural network, $i = 1, \cdots, m$; j is the output unit of the neural network, $j = 1, \cdots, n$; k is the hidden unit of the neural network, $k = 1, \cdots, p$; W_{ki} is the weight coefficient between the input neuron i and the hidden neuron k; and ω_{jk} is the output layer neuron j and the hidden neuron k. Among the weight coefficients, the absolute influence coefficient is the required weight.

5.2. Fuzzy Neural Network Training. Based on the statistics of the previous simulation results, three types of data that affect the maximum surface subsidence (Table 4) are obtained. Due to the differences in the values of the three factors, the sample data has been dimensionlessly processed, as shown in Table 5.

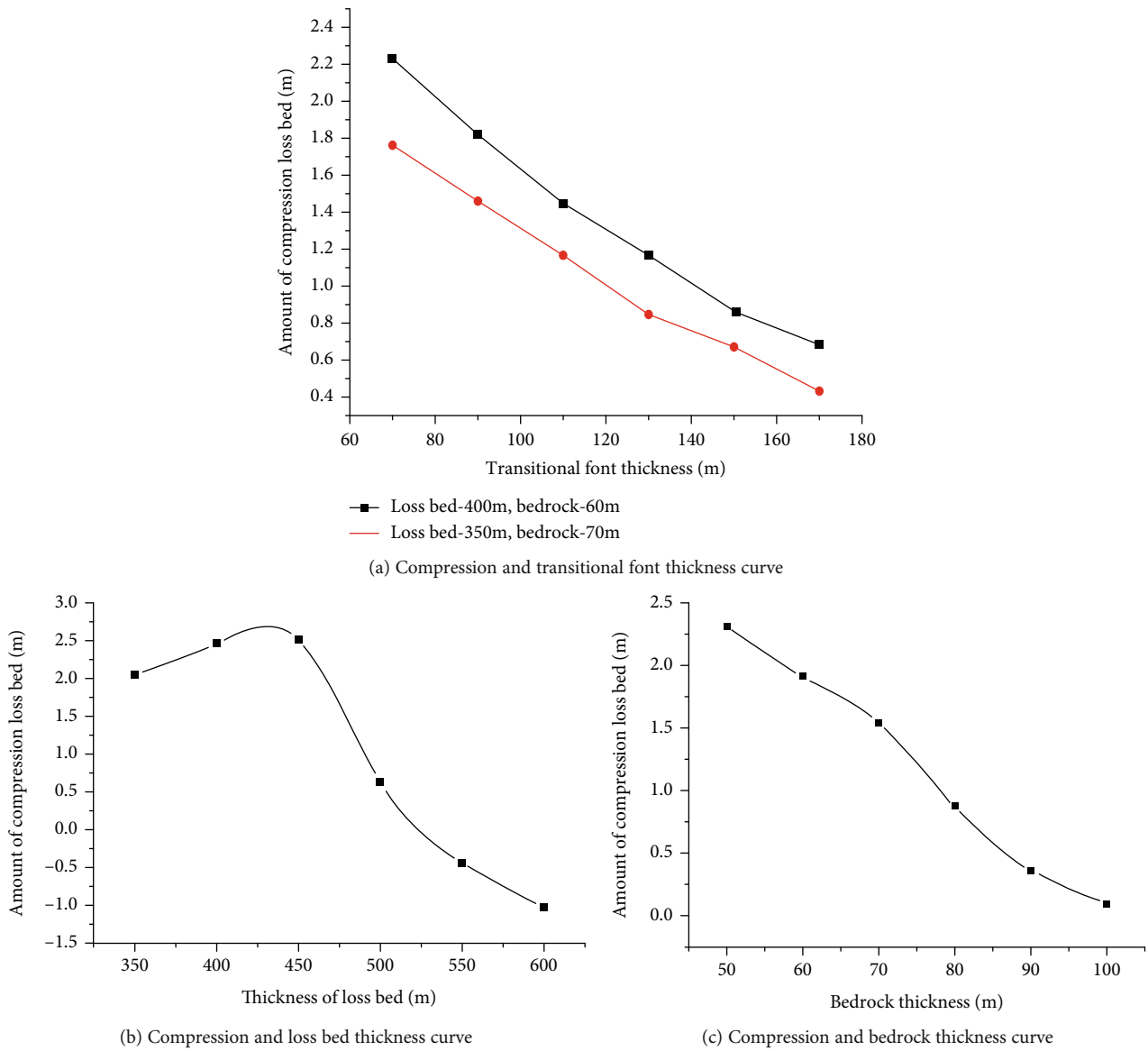

(a) Compression and transitional font thickness curve

(b) Compression and loss bed thickness curve

(c) Compression and bedrock thickness curve

Figure 16: Compression and variation of different formation factors.

Using the model to learn the sample data, the error curve is shown in Figure 19. From Figure 19, we can see that the model has a good learning effect and the accuracy of the results is high.

Based on the learning results obtained in the figure, the weight matrix is processed, and then the final weight values of the three main control factors are obtained, as shown in Table 6. Finally, the thickness of the loose layer and the transition body are calculated according to the final weight values obtained. The sensitivity ranking of the three influencing factors of bedrock thickness is shown in Table 7.

5.3. Sensitivity Analysis of Influencing Factors. It can be seen from Table 6 that the weight of the bedrock in terms of ground subsidence is the largest, reaching 0.6228; the transition body is between the bedrock and the loose layer, which is 0.2340; the weight of the loose layer is the smallest, which is 0.1432. From Table 7, it is concluded that the sensitivity of the three factors to the impact of ground subsidence is ranked as follows: bedrock > transition body > loose layer.

According to the analysis, due to the high strength of the bedrock, in the process of coal seam mining, it has a good effect on eliminating the additional stress generated by mining and supporting the overburden rock layer, restraining its movement and deformation, and reducing ground subsidence. Due to the loose nature of the loose layer, during the mining process, it cannot produce a good suppression of the subsidence and deformation of the ground surface, and the effect on the subsidence of the ground surface is relatively small. The sensitivity of the "hard soil-soft rock" transition body is between the loose layer and the bedrock, which further confirms the special nature of the transition from hard soil to soft rock, which can play a supporting role in the overlying strata. At the same time, it can restrain a part of the ground surface from sinking. Therefore, the bedrock plays a major role in controlling the surface subsidence, and the

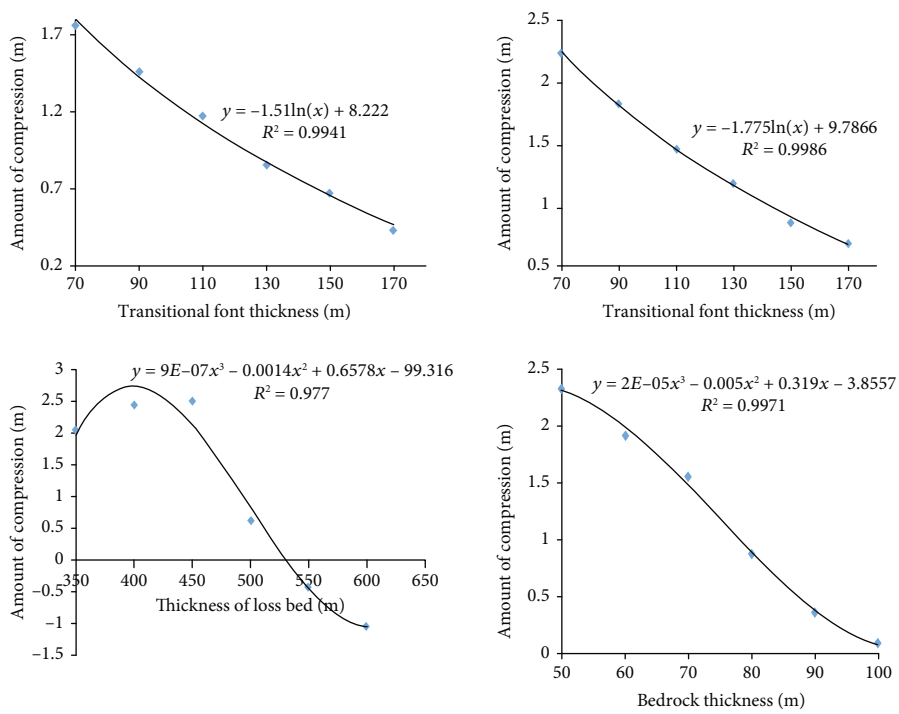

Figure 17: Compression curve and fitting curve of various factors.

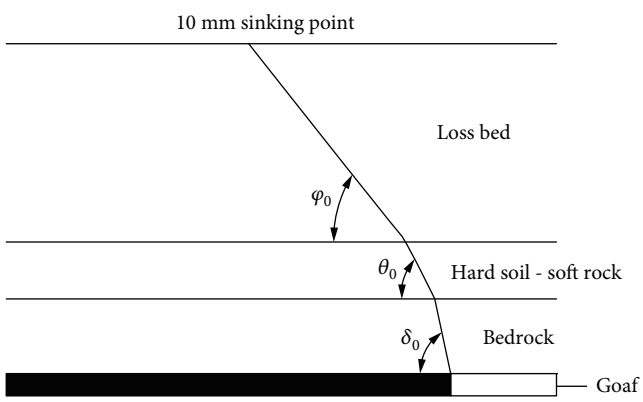

Figure 18: Boundary angle calculation diagram.

Table 3: Sinking 10 mm position.

Model number	More than 10 mm measuring point	Sinking value (mm)	Measuring point X-axis coordinate	10 mm estimated position (m)
27	5	15.8	200	177.4
28	4	17.9	160	151.9
29	3	19.8	120	118.1

transitional body also has an inhibitory effect on the surface subsidence due to the characteristics of half-soil and half-rock, and the loose layer is more consolidated than the bedrock and the transitional body. The degree is low and the nature is loose, and the effect on the surface subsidence

Table 4: Learning sample date.

Factor Program	Loose layer thickness (m)	Bedrock thickness (m)	Transition body thickness (m)	Sink value (m)
1	400	60	70	-11.21
2	400	60	90	-10.37
3	400	60	110	-9.58
4	400	60	130	-8.86
5	400	60	150	-8.15
6	400	60	170	-7.58
7	350	70	70	-10.01
8	350	70	90	-9.25
9	350	70	110	-8.56
10	350	70	130	-7.89
11	350	70	150	-7.24
12	350	70	170	-6.64
13	350	50	70	-11.03
14	400	50	70	-11.66
15	450	50	70	-11.81
16	500	50	70	-10.09
17	550	50	70	-9.23
18	600	50	70	-8.75
19	450	50	110	-11.69
20	450	60	110	-10.33
21	450	70	110	-9.15
22	450	80	110	-8.01
23	450	90	110	-7.15
24	450	100	110	-6.22

Table 5: Nondimensional treatment of learning date.

Factor Program	Loose layer thickness (m)	Bedrock thickness (m)	Transition body thickness (m)
1	0.2	0.2	0
2	0.2	0.2	0.2
3	0.2	0.2	0.4
4	0.2	0.2	0.6
5	0.2	0.2	0.8
6	0.2	0.2	1.0
7	0	0.4	0
8	0	0.4	0.2
9	0	0.4	0.4
10	0	0.4	0.6
11	0	0.4	0.8
12	0	0.4	1.0
13	0	0	0
14	0.2	0	0
15	0.4	0	0
16	0.6	0	0
17	0.8	0	0
18	1.0	0	0
19	0.4	0	0.4
20	0.4	0.2	0.4
21	0.4	0.4	0.4
22	0.4	0.6	0.4
23	0.4	0.8	0.4
24	0.4	1.0	0.4

is small. It can be seen that the influence of the "hard soil-soft rock" transition body on ground subsidence is very important, and it cannot be generalized into loose or bedrock strata. It should be divided and studied separately.

6. Case Study

The 1304N working face in a coal mining area in Shandong Province, China, was selected for the case study in this paper to investigate the surface subsidence laws and validate the results from numerical modeling analyses. Based on the field data, the thickness of the unconsolidated layer is in the range 644.8 to 655 m with an average value of 651.04 m; the thickness of the bedrock in the working face is in the range 41.6 to 76.5 m, with an average value of 59.75 m. Base on the borehole data and the theoretical analyses, the hard soil/soft rock transition zone covers a thickness of 262 m at the bottom of Neogene in the overburden unconsolidated layer of the 1304N working face, whose soil conditions are indicated in Figure 20.

The 21st observation from the observation station shows that the subsidence of P52 has exceeded 10 mm with a subsidence speed of 0.5 mm/d. The subsidence isochron shows the subsidence isochron of 10 mm passes P52, which means the high compatibility of deduced subsidence isochrons and

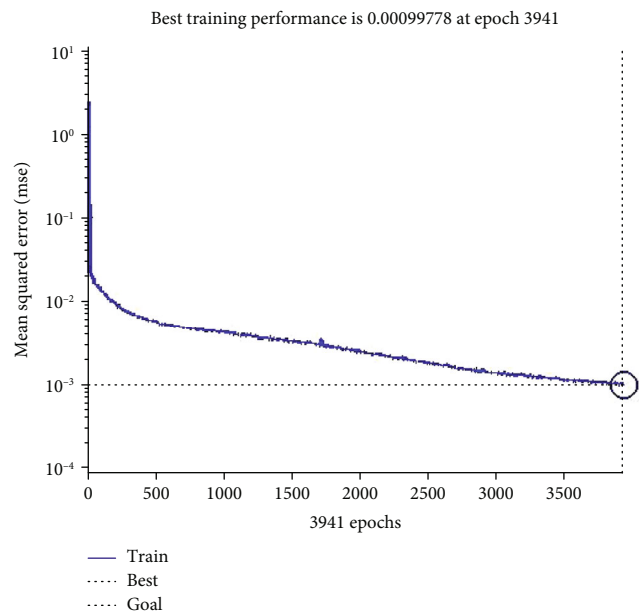

Figure 19: Fuzzy neural network training error curve.

Table 6: Contribution weight of each influence factor.

Influencing factors	Loose layer thickness	Transition body thickness	Bedrock thickness
Weights	0.1432	0.2340	0.6228

Table 7: Sensitivity ranking of each influence factor.

Influencing factors	Bedrock thickness	Transition body thickness	Loose layer thickness
Sensitivity ranking	1	2	3

those from field data. The measured distance of the boundary of mining and subsidence isochron of 10 mm in the main cross section of the 1304N strike is 606.3 m.

From the soil investigation, the thickness of the unconsolidated layer in the 1304N working face, the hard soil/soft rock transition zone, and the bedrock are 389, 262, and 61 m, respectively.

The boundary angles of the unconsolidated layer, the hard soil/soft rock transition zone, and the bedrock are 42.6°, 52.1°, and 61.3°, respectively.

$$\frac{389}{\tan\varphi_0} + \frac{262}{\tan\theta_0} + \frac{61}{\tan\delta_0} = 660.4\,\text{mm}. \tag{11}$$

The calculated distance of the boundary of mining and the subsidence isochron of 10 mm in the main cross section of the strike is 606.3 m, which is consistent with the measured value of 606.3 m, and the error is only 8.9%, suggesting a reliable result. It shows that subsidence is a creep process that lasts for a long time, and the subsidence of the 1304N working face has not reached its maximum value yet, and thus, a small error is induced.

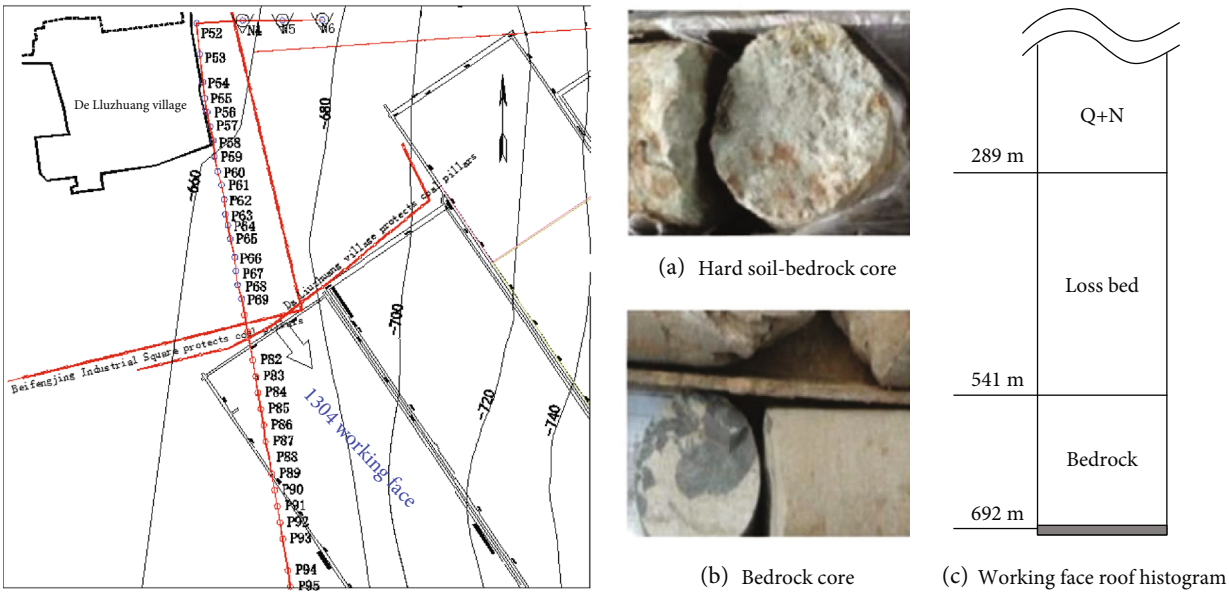

(a) Hard soil-bedrock core

(b) Bedrock core

(c) Working face roof histogram

Figure 20: Working surface formation characteristics.

7. Conclusions

The mechanism of mining subsidence caused by mining in the thick unconsolidated layer was studied in this paper. The mechanical properties of the hard soil/soft rock at the bottom of the unconsolidated layer were analyzed by means of bore holes of clay samples and laboratory tests. Numerical modeling was performed to analyze the surface subsidence in the hard soil/soft rock under different strata conditions. The main conclusions are as follows:

(1) Based on the borehole samples from several coal mining areas and analyses of mechanical behavior of the hard soil/soft rock transition block at the bottom of the unconsolidated layer, the transition is a special soil layer from which hard soil transits to soft rock, and it has an apparent influence on the mining induced surface movement. This special soil should not be treated as an unconsolidated layer nor bedrock when the surface subsidence analyses are involved

(2) The impact of different parameters (the hard soil/soft rock transition zone, the unconsolidated layer, and the thickness of bedrock) on the surface subsidence of main cross sections under different strike conditions and the characteristics of the unconsolidated layer was analyzed and studied using FLAC 3D. Numerical result shows that the hard soil/soft rock transition zone provides certain support for the overburden strata and constrains on the surface subsidence during mining, with an effective constraint effect as the depth increases. The thickness ratio of the unconsolidated layer to the bedrock only affects the degree of this constraint effects and will not cause it to disappear. The surface subsidence, as a function of the transition zone thickness, was fitted according to two different thickness ratios of the unconsolidated layer to the bedrock

(3) The boundary angle method, combined with the numerical analyses, was applied in every layer to get the boundary angle of the transition zone, which was 52.1° and in the range 42.6° (in the unconsolidated layer) to 61.3° (in the bedrock). This confirmed a transition from hard soil to soft rock

(4) The sensitivity ranking of the three factors is obtained through the neural network, and the sensitivity ranking order of bedrock > transition body > loose layer is obtained. The effect of the loose layer is the weakest

(5) The results in this study were verified with analyses of the 1340N working face in a coal mining area in Shandong Province, China

Data Availability

The data involved is confidential.

Conflicts of Interest

The authors declare no conflicts of interest.

Acknowledgments

The authors are grateful to the National Natural Science Foundation of China (51774199) and the Natural Science Foundation of Shandong Province for the support of major basic research projects (ZR2018ZC0740). Thanks are due to the Shandong New Dragon Energy Co. Ltd.

References

[1] X. E. Chen, D. H. Li, and P. F. Gou, *Mining and surface movement under thick and losses beds*, China University of Mining and Technology Press, Xuzhou, 2010.

[2] W. Yang and X. Xia, "Prediction of mining subsidence under thin bedrocks and thick unconsolidated layers based on field measurement and artificial neural networks," *Computers & Geosciences*, vol. 52, pp. 199–203, 2013.

[3] F. Wang, B. Jiang, S. Chen, and M. Ren, "Surface collapse control under thick unconsolidated layers by backfilling strip mining in coal mines," *International Journal of Rock Mechanics and Mining Sciences*, vol. 113, pp. 268–277, 2019.

[4] J. Chai, W. Lei, W. du et al., "Experimental study on distributed optical fiber sensing monitoring for ground surface deformation in extra-thick coal seam mining under ultra-thick conglomerate," *Optical Fiber Technology*, vol. 53, article 102006, 2019.

[5] Y. Sun, J. Zuo, M. Karakus, and J. Wang, "Investigation of movement and damage of integral overburden during shallow coal seam mining," *International Journal of Rock Mechanics and Mining Sciences*, vol. 117, pp. 63–75, 2019.

[6] D. Hou, D. Li, G. Xu, and Y. Zhang, "Superposition model for analyzing the dynamic ground subsidence in mining area of thick loose layer," *International Journal of Mining Science and Technology*, vol. 28, no. 4, pp. 663–668, 2018.

[7] H. Li, G. Guo, and N. Zheng, "Influence of coal types on overlying strata movement and deformation in underground coal gasification without shaft and prediction method of surface subsidence," *Process Safety and Environmental Protection*, vol. 120, pp. 302–312, 2018.

[8] J. H. Li, Y. C. Xu, P. Jiang, Y. G. Lian, and Y. Mou, "Study on load transmission characteristics of overburden rock above coal mining face in thin bedrock of super thick unconsolidated stratum," *Coal Science and Technology*, vol. 45, pp. 95–100, 2017.

[9] Y. C. Xu, S. Q. Liu, Y. B. Gao, and Q. Zhang, "Study on internal micro-deformation law of thick losses bed," *Coal Science and Technology.*, vol. 42, pp. 10–13, 2014.

[10] Y. X. Liu, H. Y. Dai, Y. D. Jiang, Y. F. Zhang, and Z. Peng, "Study on surface movement law of coal mining under deep mining with thick and loose stratum," *Coal Science and Technology*, vol. 41, pp. 117–120, 2013.

[11] D. H. Li, G. S. Xu, and H. Z. Yu, "Study on features of surface dynamic movement and deformation caused by coal mining under thick alluvium," *Coal Science and Technology*, vol. 42, pp. 103–106, 2014.

[12] J. J. Chen, Y. Chen, W. B. Guo, and Y. F. Zou, "Study on surface movement law under the condition of thick unconsolidated strata," *Coal Science and Technology*, vol. 41, pp. 95–97, 2013.

[13] J. Z. Wang, Y. S. Li, X. Zhou, L. X. Wu, and S. H. Wei, "Study on the movement law of coal surface under the super thick unconsolidated stratum," *Journal of China Coal Society*, vol. 22, pp. 20–23, 1997.

[14] L. Zhao, *Calculation of ground movement parameters and prediction of movement and deformation under the thick loose layer*, Anhui University of Science and Technology, Hefei, 2013.

[15] B. Gong, Y. Jiang, P. Yan, and S. Zhang, "Discrete element numerical simulation of mechanical properties of methane hydrate-bearing specimen considering deposit angles," *Journal of Natural Gas Science and Engineering*, vol. 76, article 103182, 2020.

[16] B. Gong, Y. Jiang, and L. Chen, "Feasibility investigation of the mechanical behavior of methane hydrate-bearing specimens using the multiple failure method," *Journal of Natural Gas Science and Engineering*, vol. 69, article 102915, 2019.

[17] J. Q. Gao, *Prediction of overburden stability in goaf of steeply inclined coal seam*, Xi'an University of Science and Technology, Xi'an, 2014.

[18] M. Marschalko, I. Yilmaz, D. Lamich et al., "Unique documentation, analysis of origin and development of an undrained depression in a subsidence basin caused by underground coal mining (Kozinec, Czech Republic)," *Environmental Earth Sciences*, vol. 72, no. 1, pp. 11–20, 2014.

[19] J. L. Cao, "Analysis on the development characteristics and influencing factors of environmental geological problems in main mines of Changzhi City," *Northwestern Geology*, vol. C00, pp. 93–96, 2003.

[20] M. Jiang, *Study on the law of overlying strata and surface movement in deep mining and wide strip mining*, Shandong University of Science and Technology, Qingdao, 2013.

[21] L. Y. Tong, S. Y. Liu, and Y. Qiu, *Hazard assessment and treatment technology of goaf under the 538 expressway*, Southeast University Press, Nanjing, 2006.

[22] W. H. Sui, *Engineering geological study on mining subsidence soil deformation*, China University of Mining and Technology Press, Xuzhou, 1999.

[23] G. L. Zhang, "Study on structural characteristics of thick loose soil in mining area," *Journal of Engineering Geology*, vol. 8, pp. 366–368, 2000.

[24] Y. S. Zhang and Y. X. Qu, "Discussion on the identification and classification of hard soil/soft rock (new type between rock and soil)," *Journal of Engineering Geology*, vol. S1, pp. 309–313, 2000.

[25] Q. X. Zhang, P. Li, and D. S. Zhao, *Soil science and soil mechanics*, Science Press, Beijing, 2005.

[26] X. Zhao, "Study on correlation of unconfined compressive strength for silty clay and clay," *Chinese Journal of Underground Space and Engineering*, vol. 9, pp. 1516–1519, 2013.

[27] Z. J. Su and W. S. Liu, "Study and application of new grouting technology for separated strata to slacken the surface subsidence," *China Safety Science Journal*, vol. 11, pp. 24–27, 2001.

[28] W. G. Xiao, *Micromechanics-based continuum method and constitutive model for jointed rock masses*, Beijing Jiaotong University, Beijing, 2011.

[29] F. P. Zhang, D. Q. Li, Z. J. Cao, T. Xiao, and J. Zhao, "Revisiting statistical correlation between Mohr-Coulomb shear strength parameters of Hoek-Brown rock masses," *Tunnelling and Underground Space Technology*, vol. 77, pp. 36–44, 2018.

[30] Y. L. Wu, "Character of cemented sand and half-diagenesis clay: a case study for the location of Xiangjiang Bridge," *Hydrogeology and Engineering Geology*, vol. 29, pp. 26–28, 2002.

[31] Z. Y. Deng, J. T. Guo, Y. G. Yan, H. Y. Dai, and Y. Chen, "The method for calculating of boundary angle and angle of critical deformation under the thick loose layer conditions," *Mining Survey*, vol. 1, article 61-63+78+4, 2011.

[32] B. Mutlu, H. A. Nefeslioglu, E. A. Sezer, M. A. Akcayol, and C. Gokceoglu, "An experimental research on the use of recurrent neural networks in landslide susceptibility mapping,"

ISPRS International Journal of Geo-Information, vol. 8, no. 12, p. 578, 2019.

[33] B. Mutlu, H. A. Nefeslioglu, E. A. Sezer, M. A. Akcayol, and C. Gokceoglu, "Ensemble neural networks for modeling DEM error," *ISPRS International Journal of Geo-Information*, vol. 8, no. 10, p. 444, 2019.

[34] L. Goulier, B. Paas, L. Ehrnsperger, and O. Klemm, "Modelling of urban air pollutant concentrations with artificial neural networks using novel input variables," *International Journal of Environmental Research and Public Health*, vol. 17, no. 6, p. 2025, 2020.